Herschel/HIFI: first science highlights

Astronomy & Astrophysics

Special feature

HIFI spectroscopy of low-level water transitions in M 82[*]

A. Weiß[1], M. A. Requena-Torres[1], R. Güsten[1], S. García-Burillo[2], A. I. Harris[3], F. P. Israel[4], T. Klein[1], C. Kramer[5], S. Lord[6], J. Martin-Pintado[7], M. Röllig[8], J. Stutzki[8], R. Szczerba[9], P. P. van der Werf[4], S. Philipp-May[1], H. Yorke[10], M. Akyilmaz[8], C. Gal[8], R. Higgins[13], A. Marston[12], J. Roberts[7], F. Schlöder[8], M. Schultz[8], D. Teyssier[12], N. Whyborn[11], and H. J. Wunsch[1]

[1] Max-Planck-Institut für Radioastronomie, Auf dem Hügel 69, 53121 Bonn, Germany
   e-mail: aweiss@mpifr-bonn.mpg.de
[2] Observatorio Astronomico Nacional (OAN) – Observatorio de Madrid, Alfonso XII 3, 28014 Madrid, Spain
[3] Department of Astronomy, University of Maryland, College Park, MD 20742, USA
[4] Leiden Observatory, Leiden University, PO Box 9513, 2300 RA Leiden, The Netherlands
[5] IRAM, Avenida Divina Pastora 7, 18012 Granada, Spain
[6] NASA *Herschel* Science Center, Caltech, Pasadena, CA, USA
[7] Centro de Astrobiologia (INTA-CSIC), Ctra de Torrejon a Ajalvir, km 4, 28850 Torrejon de Ardoz, Madrid, Spain
[8] KOSMA, I. Physikalisches Institut der Universität zu Köln, Zülpicher Strasse 77, 50937 Köln, Germany
[9] N. Copernicus Astronomical Center, Rabiańska 8, 87-100 Toruń, Poland
[10] Jet Propulsion Laboratory, 4800 Oak Grove Drive, Pasadena, California 91109, USA
[11] Atacama Large Millimeter/Submillimeter Array, Joint ALMA Office, Santiago, Chile
[12] European Space Astronomy Centre, ESA, PO Box 78, 28691 Villanueva de la Cañada, Madrid, Spain
[13] Experimental Physics Dept., National University of Ireland Maynooth, Co. Kildare, Ireland

ABSTRACT

We present observations of the rotational ortho-water ground transition, the two lowest para-water transitions, and the ground transition of ionised ortho-water in the archetypal starburst galaxy M 82, performed with the HIFI instrument on the *Herschel* Space Observatory. These observations are the first detections of the para-$H_2O(1_{11}-0_{00})$ (1113 GHz) and ortho-$H_2O^+(1_{11}-0_{00})$ (1115 GHz) lines in an extragalactic source. All three water lines show different spectral line profiles, underlining the need for high spectral resolution in interpreting line formation processes. Using the line shape of the para-$H_2O(1_{11}-0_{00})$ and ortho-$H_2O^+(1_{11}-0_{00})$ absorption profile in conjunction with high spatial resolution CO observations, we show that the (ionised) water absorption arises from a ~2000 pc^2 region within the HIFI beam located about ~50 pc east of the dynamical centre of the galaxy. This region does not coincide with any of the known line emission peaks that have been identified in other molecular tracers, with the exception of HCO. Our data suggest that water and ionised water within this region have high (up to 75%) area-covering factors of the underlying continuum. This indicates that water is not associated with small, dense cores within the ISM of M 82 but arises from a more widespread diffuse gas component.

Key words. line: formation – galaxies: ISM – ISM: molecules – galaxies: individual: M 82 – infrared: galaxies – submillimeter: galaxies

1. Introduction

High-resolution spectroscopy of far-infrared and sub-millimetre water lines is an important tool for studying the physical and chemical properties of the interstellar medium (ISM). Absorption by terrestrial atmospheric water vapour has ground-based studies of water in extragalactic systems limited to radio maser transitions (such as the famous 22 GHz water line) or to a few systems with significant redshift (e.g. Combes & Wiklind 1997; Cernicharo et al. 2006; Menten et al. 2008). Earlier satellite missions, such as *Odin* and SWAS, did not have enough collecting area to detect the relatively faint ground transitions of water in external galaxies. ISO and, more recently, *Spitzer* have provided the first systematic studies of water in the far infrared (IR) regime (e.g. Fischer et al. 1999; Gonzalez-Alfonso 2004). These missions, however, did not cover the frequencies of the water ground transitions and other low-level water lines.

Only with the launch of the *Herschel* satellite, with its large collecting area, have these transitions become accessible in the nearby universe (e.g. van der Werf et al. 2010). As part of the HEXGAL guaranteed time key program (PI Güsten), we are surveying the low-level water lines in different nuclear environments, performing velocity-resolved spectroscopy with the Heterodyne Instrument for the Far Infrared (HIFI, de Graauw et al. 2010). In this letter we report on our first observations towards the central region of the archetypal starburst galaxy M 82. We adopt a distance of 3.9 Mpc (Sakai & Madore 1999).

2. Observations and data reduction

Using the HIFI instrument onboard *Herschel*, we have observed the ground transitions of ortho and para water, o-$H_2O(1_{10}-1_{01})$ and p-$H_2O(1_{11}-0_{00})$, as well as the p-$H_2O(2_{02}-1_{11})$ line, towards the centre of M 82 (RA = $09^h55^m52\overset{s}{.}22$ Dec = $69°40'46\overset{''}{.}9$ J2000). Observations were carried out in fast-chopping dual-beamswitch mode using a wobbler throw of 3′ for all observations. The wobbler frequency was 0.8, 1.4, and 2.0 Hz for the 557 GHz, 988 GHz, and 1113 GHz observations, respectively. Nodding was performed every ~40 s. Calibration was achieved through hot/cold absorber measurements every 20 min. The data were recorded using the wide-band acousto-optical spectrometer, consisting of four units with a bandwidth of 1 GHz each, covering the 4 GHz IF for each polarization with spectral resolution of 1 MHz.

Data were reduced using the HIPE[1] and CLASS[2] software packages. Spectra were calibrated using HIPE and then exported to CLASS format with the shortest possible pre-integration (typically ~40 s). For each scan we combined the four sub-bands in each polarization to create a 4 GHz spectrum. From this spectrum we computed the underlying continuum using the line-free channels; we then subtracted first-order baselines from individual sub-bands. The baseline-subtracted sub-bands were again combined and the continuum level added. This results in a noise-weighted 4 GHz spectrum for each scan. These spectra were inspected for remaining baseline instabilities, and scans with distorted baselines were omitted. For each line we inspected the co-added result in both polarizations (H and V) separately. The continuum level was found to agree better than 10% for each frequency. The integrated line intensities agree within 25% without significant differences of the line profiles (although the latter comparison is limited by the signal-to-noise ratio, in particular for the 557 GHz observations). In the following we therefore use the noise-weighted average of both polarizations, which yields effective on-source integration times for the three lines are 750, 2250, and 1300 s for the o-$H_2O(1_{10}-1_{01})$, p-$H_2O(1_{11}-0_{00})$, and p-$H_2O(2_{02}-1_{11})$ lines, respectively.

Since HIFI's calibration is still preliminary, we used the theoretical predictions based on the *Herschel's* expected surface accuracy and the geometrical aperture size to convert the antenna temperatures to flux density (Kramer 2006). This yields 462 Jy K^{-1}, 467 Jy K^{-1}, and 470 Jy K^{-1} at 557 GHz, 988 GHz, and 1113 GHz, respectively. The final spectra are shown at a velocity resolution of 20, 10, and 25 km s^{-1} in Fig. 1 (top).

3. Results

All three water lines have been detected with high significance, demonstrating that faint (few mK) broad lines can be observed with HIFI. The o-$H_2O(1_{10}-1_{01})$ line is detected in emission and shows a double-peaked line profile. Within noise uncertainty, no emission (or absorption) is detected on the systemic velocity of M 82 (v_{LSR} = 225 km s^{-1}). Both components are well fit by Gaussian profiles, with line parameters given in Table 1. We detect a continuum level of 12.8 Jy beam^{-1} at 557 GHz.

Our 1113 GHz spectrum shows two absorption features, one centered at the systemic velocity of M 82 corresponding to the p-$H_2O(1_{11}-0_{00})$ line, and a second stronger feature blue-shifted by ~1.8 GHz with respect to the systemic velocity. We identify the blue-shifted absorption feature as o-$H_2O^+(1_{11}-0_{00})$

(ν_{rest} = 1115.186 GHz, Mürtz et al. 1998). Both absorption line profiles are identical within the uncertainties (see Fig. 2). The absorption profile is approximated reasonably well by a single Gaussian (see Table 1 for the line parameters). The continuum level detected at 1113 GHz is 78 Jy beam^{-1}.

The p-$H_2O(2_{02}-1_{11})$ line at 988 GHz is detected in emission. Its line profile differs from both the o-$H_2O(1_{10}-1_{01})$ emission profile and the p-$H_2O(1_{11}-0_{00})$ absorption profiles. It shows emission between v_{LSR} = 50−500 km s^{-1} (similar to the velocity range covered by CO at the same spatial resolution, see below) and is almost flat-topped for velocities between 100 and 400 km s^{-1}. Thus the spectrum does not indicate absorption (or absence of emission) at the systemic velocity. The spectrum can be decomposed into two Gaussian profiles, with parameters given in Table 1. The continuum flux detected at 988 GHz is 61 Jy beam^{-1}.

4. Discussion

4.1. The line profiles

Given the large body of high spatial resolution observations of molecular gas tracers published for M 82, the line profile of the water lines can be compared to other data to learn more about the location and extent of the water emitting/absorbing regions in the disk. We here compare the water line profiles to the high spatial resolution (3.5″) ^{12}CO($J = 1 \rightarrow 0$) data cube obtained by Walter et al. (2002); ^{12}CO (CO thereafter) is the best-studied tracer of the molecular gas in M 82. We first compare the CO spectra in beams synthesized to the same spatial resolutions as the HIFI beams. From the comparison of the p-$H_2O(1_{11}-0_{00})$ absorption spectrum to CO, it is apparent that the absorption is not only detected in the pronounced absorption feature close to the systemic velocity, but also at velocities in the wings of the CO profile (Fig. 1 bottom). It is therefore tempting to speculate that the lack of absorption at certain velocities has a geometrical origin, i.e., that gas at these velocities is located behind the continuum. This is also supported by the shape of the p-$H_2O(2_{02}-1_{11})$ line emission profile, which shows that water is abundant in the gas phase of M 82 at all velocities where CO (i.e. molecular gas) is present. The very good correspondence of the o-$H_2O^+(1_{11}-0_{00})$ absorption profile near the systemic velocity suggests that the ionised water traces the same gas as is detected in the water absorption. A closer inspection of the o-$H_2O^+(1_{11}-0_{00})$ profile shows, however, a lack of absorption in the red wing of the line profile (see Fig. 2). The blue wing is only partly covered by our spectrum and shows emission at the very blue edge. This could come from calibration uncertainties at the edge of the IF-band, but it is unclear whether this feature is an artifact or is real.

Our finding that the p-$H_2O(1_{11}-0_{00})$ line is observed in absorption while the p-$H_2O(2_{02}-1_{11})$ line is detected in emission can be used to obtain an estimate of the excitation temperatures of both lines. We used the dust model by Siebenmorgen & Krügel (2007) to estimate a background temperature of 18 K and 20 K at 988 and 1113 GHz, respectively. This implies T_{ex} < 20 K for p-$H_2O(1_{11}-0_{00})$ and T_{ex} > 18 K for p-$H_2O(2_{02}-1_{11})$ (or $T_{ex} \approx 19$ K if both lines are close to LTE). Given the complexity of the water energy level diagram and the various level population channels (collisional or radiative), detailed models will be required for investigating the underlying excitation mechanisms.

Owing to the much larger beam size of the o-$H_2O(1_{10}-1_{01})$ observations, a comparison to the other water lines is not straightforward. In comparison to CO, however, it is apparent that the o-$H_2O(1_{10}-1_{01})$ emission arises exclusively from
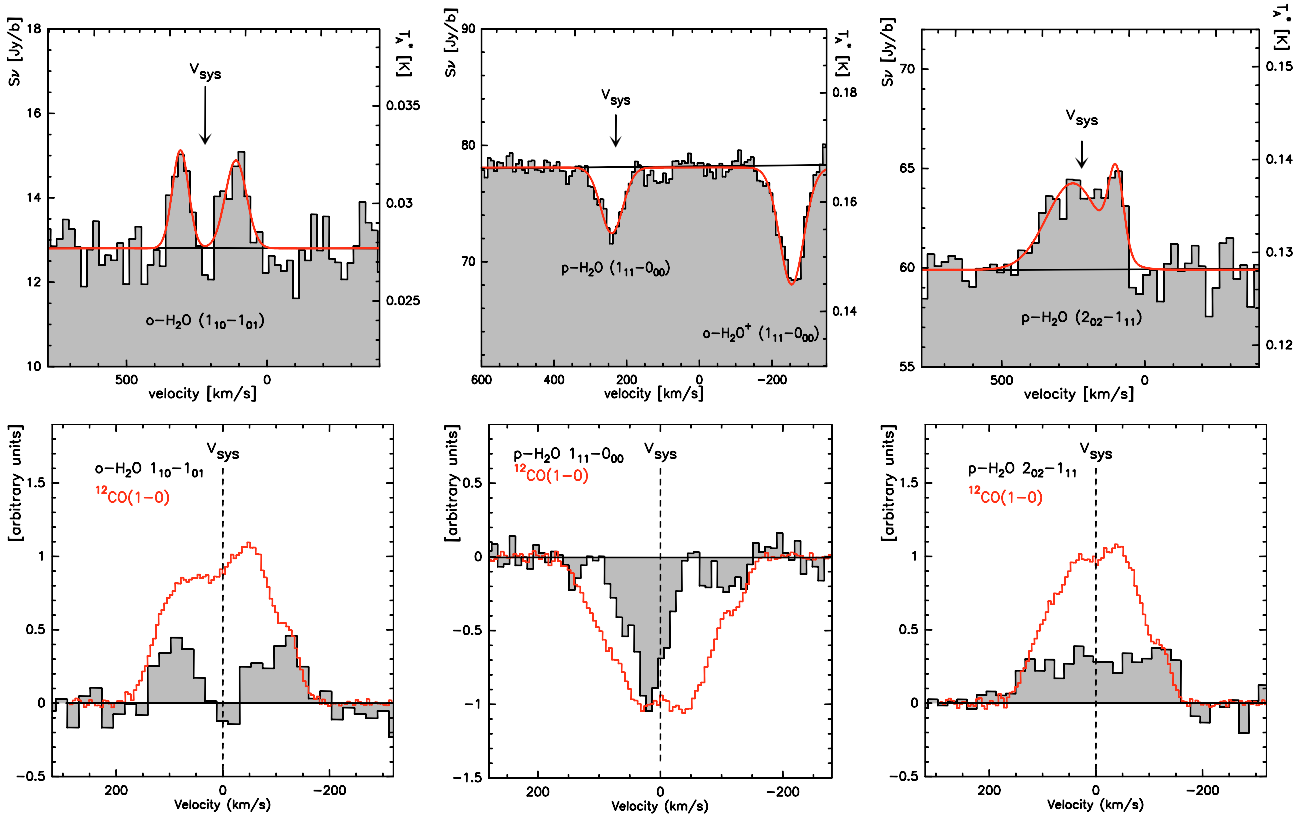
Fig. 1. *Top*: spectra of the o-$H_2O(1_{10}-1_{01})$, p-$H_2O(1_{11}-0_{00})$ and p-$H_2O(2_{02}-1_{11})$ lines towards the centre of M 82, with Gaussian-fit profiles superposed. The line parameters are given in Table 1. *Bottom*: water-line profiles superposed on the CO($J = 1 \rightarrow 0$) line profiles within beams synthesized with the same spatial resolution as the water data. The velocity scale is relative to the systemic velocity of M 82 ($v_{LSR} = 225$ km s^{-1}). The intensities of the CO line profiles have been normalized to unity, and the water line profiles scaled to provide close matches to the CO profiles in the line wings. The CO profile in *the middle panel* has been inverted for better comparison to the water absorption profile.

Table 1. Line parameters derived from a Gaussian fit.

Line	ν_{rest} [GHz]	beam size ['']	T_A^* peak [mK]	S_ν peak [Jy beam^{-1}]	I_ν [Jy beam^{-1} km s^{-1}]	v_{LSR} [km s^{-1}]	dv [km s^{-1}]	S_ν cont. [Jy beam^{-1}]
o-$H_2O(1_{10}-1_{01})$	556.936	41	4.5 ± 1.1	2.1 ± 0.5	200 ± 33	110 ± 8	90 ± 15	12.8 (540 μm)
			5.0 ± 1.1	2.3 ± 0.5	170 ± 29	308 ± 6	68 ± 11	
p-$H_2O(2_{02}-1_{11})$	987.927	23	8.9 ± 2.0	4.2 ± 0.9	273 ± 90	100 ± 9	61 ± 20	60.0 (300 μm)
			9.3 ± 2.0	4.4 ± 0.9	1005 ± 130	250 ± 15	220 ± 27	
p-$H_2O(1_{11}-0_{00})$	1113.343	20	-12.0 ± 1.6	-5.6 ± 0.7	-432 ± 28	240 ± 2	72 ± 6	78.1 (270 μm)
o-$H_2O^+(1_{11}-0_{00})$	1115.186	20	-21.4 ± 1.6	-10.1 ± 0.7	-836 ± 29	242 ± 2	77 ± 5	

velocities in the line wings of the CO spectrum. These velocities mainly correspond to emission in the southwestern and northeastern molecular lobes that are located within the 41'' beam (see Fig. 3 for the CO distribution compared to the HIFI beams), and yet we cannot rule out that the lack of o-$H_2O(1_{10}-1_{01})$ emission near the systemic velocities is due to self absorption in the water line profile. Observations of the water lines within the molecular lobes will be required to obtain similar spatial coverage of all lines, thus allowing detailed analysis of different line profiles and modeling of the water excitation. These observations have been approved and will be presented in a forthcoming paper.

We retrieved sub-beam location information by comparing CO line profiles at the highest spatial resolution (3.5'') to the p-$H_2O(1_{11}-0_{00})$ and o-$H_2O^+(1_{11}-0_{00})$ line profiles. The results are displayed in Fig. 3, where we show selected CO spectra overlaid on the p-$H_2O(1_{11}-0_{00})$ absorption profile. We find that the CO line profile is in very good agreement with the water absorption profile in only a small region within the HIFI beam.

The region delineated in Fig. 3 corresponds to a small strip orthogonal to the molecular disk of M 82. The CO profiles east and west of this region show significant shifts of their line centroids compared to the peak of the water absorption due to the rotation of the molecular disk. Interestingly, the CO line profiles that match the shape of the main water absorption profile also show a blue wing. This CO emission corresponds to molecular gas in the outflow of M 82 (Walter et al. 2002). This shows that the water absorption in the blue line wing arises not only from the northwestern molecular lobe (which has similar velocities and is at least partly covered by the HIFI beam), but also from gas in the outflow.

4.2. The origin of the H_2O/H_2O^+ absorption

We used the observed absorption depth to investigate whether the p-$H_2O(1_{11}-0_{00})$ and o-$H_2O^+(1_{11}-0_{00})$ absorption arises from small cores or from a more widespread gas phase of the ISM.
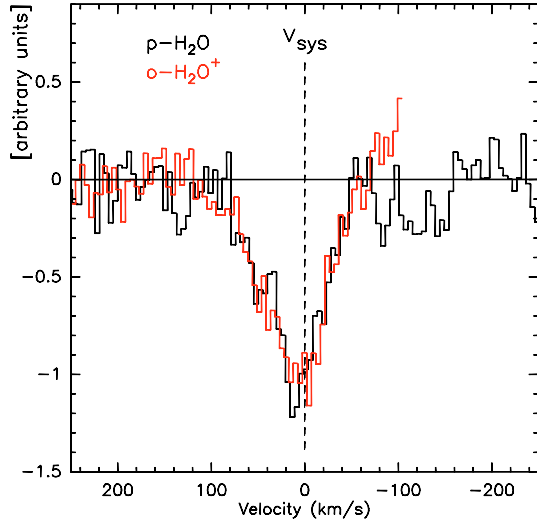
Fig. 2. Line profiles of the p-$H_2O(1_{11}-0_{00})$ (black) and the o-$H_2O^+(1_{11}-0_{00})$ (red) lines. The velocity scale is relative to the systemic velocity of M 82. Both profiles have been normalized to a maximum absorption of unity.
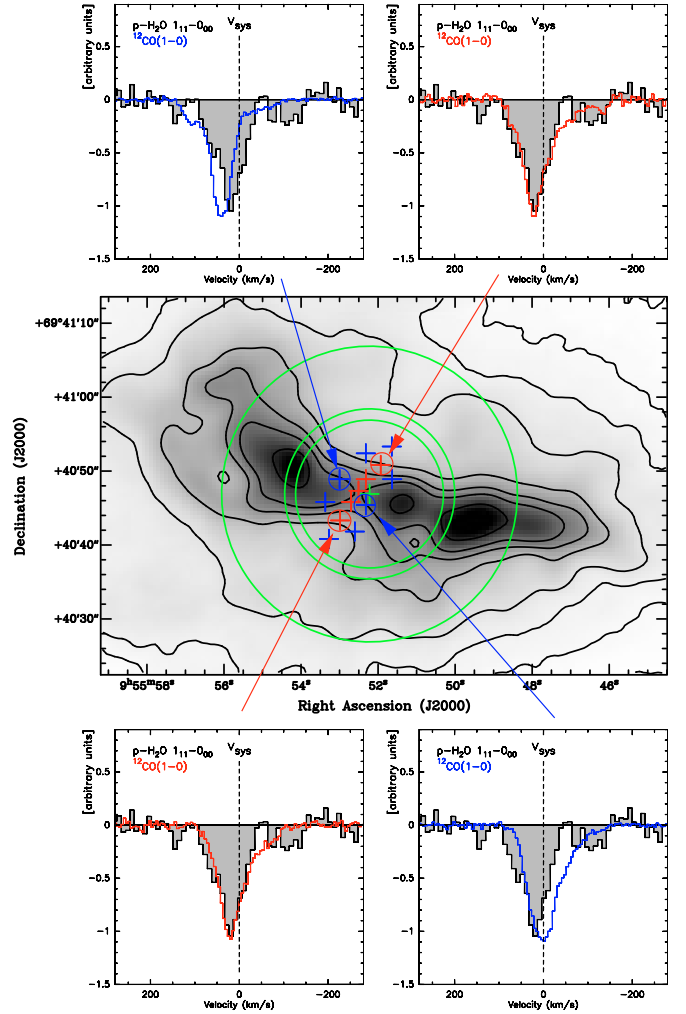

Fig. 3. HIFI beam sizes (*FWHM*) for our observing frequencies shown on the integrated CO($J = 1 \rightarrow 0$) distribution (Walter et al. 2002) in the central region of M 82. The green cross indicates our pointing centre which corresponds to the dynamical centre of M 82. The red crosses indicate the locations where the CO profiles at 3.5″ resolution match the p-$H_2O(1_{11}-0_{00})$ absorption profiles, and the blue crosses indicate locations where the CO profile significantly differs. The spectra to the top and bottom show example CO spectra superposed on the water absorption profiles. Their positions have also been marked by a circle for better visualization.

For this we assume that both lines are optically thick. This implies that the absorption depth directly measures the continuum covering factor, once the continuum distribution is known. We here use the 3 mm continuum shown in Fig. 4 as a proxy for the submm continuum distribution. Although the continuum at this wavelength is not automatically a good indicator of the thermal dust emission, because of possible free-free contamination, the spatial similarity between the the 3 mm and radio continua at high spatial resolution, as well as the similarity of the 3 mm if smoothed to similar resolution to the published 350 μm maps (Leeuw & Robson 2009), justifies this approach. The total continuum emission of M 82 at 1113 GHz was estimated using the dust model by Siebenmorgen & Krügel (2007). Combining this with the observed 3 mm continuum distribution, we estimate $S_{1113\,GHz} = 13.5$ Jy within the region of the water absorption. This translates into a continuum covering factor of 40% for p-$H_2O(1_{11}-0_{00})$ and 75% for o-$H_2O^+(1_{11}-0_{00})$. This approach yields predicted continuum fluxes within the HIFI beams that agree within 10% or better with the observed continuum fluxes listed in Table 1 at all three frequencies. Since the water absorption region covers ~2000 pc^2, these numbers strongly suggest that the p-$H_2O(1_{11}-0_{00})$ and o-$H_2O^+(1_{11}-0_{00})$ absorption arise from a widespread gas phase of the ISM and not from dense cores (which are expected to cover a much smaller fraction of the continuum). Considering the high critical densities for collisional excitation of water (a few times 10^7 cm^{-3}, Faure et al. 2007), this also implies that the water excitation cannot be driven by collisions, but is most likely dominated by the IR field. This conclusion agrees with findings in other IR bright galaxies such as Arp 220 and Mrk 231 (e.g. Gonzalez-Alfonso et al. 2004; Gonzalez-Alfonso et al. 2010).

We can also use the absorption depth to calculated the absorbing gas column densities assuming that the absorption is not intrinsically saturated and using the continuum strength derived above (13.5 Jy). Applying the method by Menten et al. (2008) we derive $\int \tau_{app} dv$ of 38.6 km s^{-1} and 107.2 km s^{-1} from the p-$H_2O(1_{11}-0_{00})$ and o-$H_2O^+(1_{11}-0_{00})$ absorption profiles. With the low-excitation temperature approximation, $N_l = \frac{8\pi v^3}{A_{ul}c^3} \frac{g_l}{g_u} \int \tau_{app} dv$, this yields ground-level column densities of

N(p–H_2O 000) = 9.0×10^{13} cm^{-2} and N(o–H_2O^+ 000) = 2.2×10^{14} cm^{-2}. For the latter, the fine structure splitting of o-H_2O^+ (see e.g. Ossenkopf et al. 2010) has been taken into account. Assuming an ortho-to-para ratio of 3:1 this results in lower limits for the total column densities of N(H_2O) $\geq 3.6 \times 10^{14}$ cm^{-2} and N(H_2O^+) $\geq 2.9 \times 10^{14}$ cm^{-2}. By converting the measured CO intensities in the absorption region to proton column densities using an X_{CO} conversion factor as given in Walter et al. (2002), we derive limits for the fractional abundances of [H_2O] $\geq 4.0 \times 10^{-9}$ and [H_2O^+] $\geq 3.3 \times 10^{-9}$. These numbers are 2–3 mag lower than the water abundances derived for Arp 220 and Mrk 231 (~10^{-6}, Gonzalez-Alfonso et al. 2004; Gonzalez-Alfonso et al. 2010), but approach values found in molecular cloud cores, the diffuse gas in the Milky Way, and in the $z = 0.89$ absorption system PKS 1830-211 (e.g. Snell et al. 2000; van der Tak et al. 2010; Menten et al. (2008).
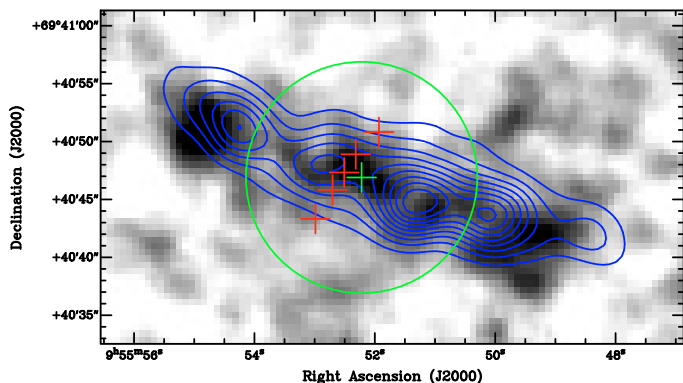
Fig. 4. 3mm continuum emission (blue contours, Weiß et al. 2001a) superposed on the integrated HCO distribution (grayscale, García-Burillo et al. 2002). The green circle indicates the *FWHM* of the HIFI beam at the p-$H_2O(1_{11}-0_{00})$ frequency, the red crosses indicate the region of the water absorption as derived based on the CO line profiles (see Fig. 3).

4.3. Comparison to other molecular gas tracers

As shown in Fig. 3 the water absorption region is not associated with a particular CO-bright region in M 82, but is located between the northeastern molecular lobe and the central CO peak. This indicates that the water absorption is not associated with the bulk of the molecular gas in M 82 or that the underlying continuum distribution favors an absorption in regions that are not bright in CO. The latter can be ruled out by comparing the spatial distribution of the water absorption to the radio (Wills et al. 1997) and mm-continuum (Weiß et al. 2001a) as a proxy for the spatial distribution of the submm continuum (e.g. using the FIR-radio correlation). Neither tracer provides evidence that the submm continuum is in particular pronounced towards the region of the water absorption (see Fig. 4), which suggests that the small size of the water absorption is related to the ISM properties rather than to the continuum distribution.

We have further compared the spatial distribution of the dense gas as traced by HCN (Brouillet & Schilke 1993) and $H^{13}CO^+$ (García-Burillo et al. 2002) to the water absorption region. These tracers, however, closely follow the distribution of the CO emission, which rules out any interpretation that the water absorption occurs predominantly in high-density regions.

A possible mechanism to efficiently release water from dust grains into the gas phase are shocks (e.g. Cernicharo et al. 1999). A comparison to the SiO distribution in M 82 (García-Burillo et al. 2001) shows that there is no indication of strong shocks in this particular region. The SiO observations, however, do not rule out the possibility that weaker C-type shocks could release H_2O efficiently from the dust grains into the gas phase without disrupting the grains themselves. In this context it is interesting to note that the water absorption is located near the expected location of the x2 orbits (and their intersection with the x1 orbits) proposed in the context of gas motions in the stellar bar potential of M 82 (e.g. Greve et al. 2002). Shocks associated with the orbital intersection would provide a plausible mechanism for releasing water into the gas phase, and the geometry of the orbits would naturally explain why the absorption is only detected to the east of the dynamical centre of M 82 (see Fig. 2 in Greve et al. 2002).

On the other hand molecular abundances in M 82 are thought to be largely influenced by chemistry in photon-dominated regions (PDRs, see e.g. Martin et al. 2006). UV photons photodissociate water and PDR models predict that significant water

gas phase abundances should only be present in well-shielded, high column density regions (see e.g. Meijerink & Spaans 2005). This interpretation is challenged by our finding that the water absorption region in M 82 is located in a relatively low column density region within the disk of M 82. Furthermore the water absorption coincides with a peak of the spatial distribution of HCO (García-Burillo et al. 2002, see Fig. 4). HCO is a tracer of PDRs, and it is the only molecule so far imaged at high spatial resolution that shows enhanced emission in this region. The similarity of the p-$H_2O(1_{11}-0_{00})$ and o-$H_2O^+(1_{11}-0_{00})$ absorption profiles shows that ionizing photons are present in the absorbing medium. Therefore UV dissociation could suppress the water gas phase abundances, leading to much lower water abundances in M 82 compared to those derived in Arp 220 and Mrk 231. This is in line with studies of other molecules with low ionization potential, such as as NH_3 and HNCO, for which photo dissociation has been suggested as a main driver for the low abundances observed in M 82 (Weiß et al. 2001b; Martin et al. 2009).

References

Brouillet, N., & Schilke, P. 1993, A&A, 277, 381
Cernicharo, J., Pardo, J. R., Gonzalez-Alfonso, E., et al. 1999, ApJ, 520, L131
Cernicharo, J., Pardo, J. R., & Weiß, A. 2006, ApJ, 646, 49
Combes, F., & Wiklind, T. 1997, ApJ, 486, 79
de Graauw, Th., Helmich, F. P., Phillips, T. G., et al. 2010, A&A, 518, L6
Faure, A., Crimier, N., Ceccarelli, C., et al. 2007, A&A, 472, 1029
Fischer, J., Luhman, M. L., Satyapal, S., et al. 1999, Ap&SS, 266, 91
García-Burillo, S., Martin-Pintado, J., Fuente, A., & Neri, R. 2001, ApJ, 563, 27
García-Burillo, S., Martin-Pintado, J., Fuente, A., Usero, A., & Neri, R. 2002, ApJ, 575, 55
Greve, A., Wills, K. A., Neininger, N., & Pedlar, A. 2002, A&A, 383, 56
Gonzalez-Alfonso, E., Smith, H. A., Fischer, J., & Cernicharo, J. 2004, ApJ, 613, 247
Gonzalez-Alfonso, E., Fischer, J., Isaak, K., et al. 2010, A&A, 518, L43
Kramer, C., Spatial Response – Contribution to the framework document of the HIFI/*Herschel* calibration group, HIFI/ICC/2003-30, version 1.8 (May 2006)
Leeuw, L. L., & Robson, E. 2009, AJ, 137, 517
Martín, S., Mauersberger, R., Martín-Pintado, J., Henkel, C., & García-Burillo, S. 2006, ApJS, 164, 450
Martín, S., Martín-Pintado, J., & Mauersberger, R. 2009, ApJ, 694, 610
Meijerink, R., & Spanns, M. 2005, A&A, 436, 397
Menten, K., Güsten, R., Leurini, S., et al. 2008, A&A, 492, 725
Mürtz, P., Zink, L. R., Evenson, K. M., & Brown, J. M. 1998, JChPh, 109.9744
Ossenkopf, V., Müller, H. S. P., Lis, D. C., et al. 2010, A&A, 518, L111
Sakai, S., & Madore, B. F. 1999, ApJ, 526, 599
Siebenmorgen, R., & Krügel, E. 2007, A&A, 461, 445
Snell, R. L., Howe, J. E., Ashby, M. L. N., et al. 2000, ApJ, 539, 101
van der Tak, F. F. S., Marseille, M. G., Herpin, F., et al. 2010, A&A, 518, L107
Van der Werf, P. P., Isaak, K. G., Meijerink, R., et al. 2010, A&A, 518, L42
Walter, F., Weiß, A., & Scoville, N. Z. 2002 , ApJ, 580, 21
Wills, K. A., Pedlar, A., Muxlow, T. W. B., & Wilkinson, P. N. 1997, MNRAS, 291, 517
Weiß, A., Neininger, N., Hüttemeister, S., & Klein, U. 2001a, A&A, 365, 571
Weiß, A., Neininger, N., Henkel, C., Stutzki, J., & Klein, U. 2001b, ApJ, 554, 143